POLITECNICO DI TORINO
Repository ISTITUZIONALE

Molecular Factors Controlling the Isomerization of Azobenzenes in the Cavity of a Flexible Coordination Cage

Original
Molecular Factors Controlling the Isomerization of Azobenzenes in the Cavity of a Flexible Coordination Cage / Pesce, Luca; Perego, Claudio; Grommet, Angela B; Klajn, Rafal; Pavan, Giovanni M. - In: JOURNAL OF THE AMERICAN CHEMICAL SOCIETY. - ISSN 0002-7863. - 142:21(2020), pp. 9792-9802. [10.1021/jacs.0c03444]

Availability:
This version is available at: 11583/2830272 since: 2020-11-23T15:02:44Z

Publisher:
AMERICAN CHEMICAL SOCIETY

Published
DOI:10.1021/jacs.0c03444

Terms of use:

This article is made available under terms and conditions as specified in the corresponding bibliographic description in the repository

Publisher copyright

(Article begins on next page)

07 May 2026

This is an open access article published under a Creative Commons Non-Commercial No Derivative Works (CC-BY-NC-ND) Attribution License, which permits copying and redistribution of the article, and creation of adaptations, all for non-commercial purposes.

ACS AUTHORCHOICE

JACS
JOURNAL OF THE AMERICAN CHEMICAL SOCIETY

pubs.acs.org/JACS

Article

Molecular Factors Controlling the Isomerization of Azobenzenes in the Cavity of a Flexible Coordination Cage

Luca Pesce, Claudio Perego, Angela B. Grommet, Rafal Klajn, and Giovanni M. Pavan*

Cite This: J. Am. Chem. Soc. 2020, 142, 9792−9802

Read Online

ACCESS | Metrics & More | Article Recommendations | Supporting Information

ABSTRACT: Photoswitchable molecules are employed for many applications, from the development of active materials to the design of stimuli-responsive molecular systems and light-powered molecular machines. To fully exploit their potential, we must learn ways to control the mechanism and kinetics of their photoinduced isomerization. One possible strategy involves confinement of photoresponsive switches such as azobenzenes or spiropyrans within crowded molecular environments, which may allow control over their light-induced conversion. However, the molecular factors that influence and control the switching process under realistic conditions and within dynamic molecular regimes often remain difficult to ascertain. As a case study, here we have employed molecular models to probe the isomerization of azobenzene guests within a Pd(II)-based coordination cage host in water. Atomistic molecular dynamics and metadynamics simulations allow us to characterize the flexibility of the cage in the solvent, the (rare) guest encapsulation and release events, and the relative probability/kinetics of light-induced isomerization of azobenzene analogues in these host−guest systems. In this way, we can reconstruct the mechanism of azobenzene switching inside the cage cavity and explore key molecular factors that may control this event. We obtain a molecular-level insight on the effects of crowding and host−guest interactions on azobenzene isomerization. The detailed picture elucidated by this study may enable the rational design of photoswitchable systems whose reactivity can be controlled via host−guest interactions.

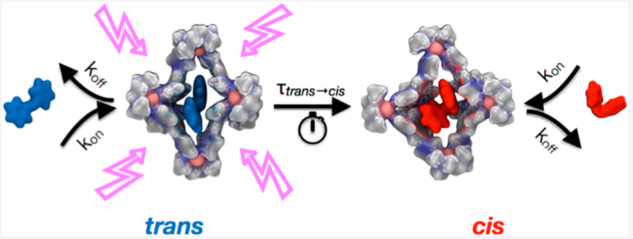

INTRODUCTION

Photochromic molecular switches such as azobenzene,[1] spiropyran,[2,3] or arylazopyrazole[4,5] are responsive molecules that isomerize upon irradiation with light. Achieving fine control of these compounds' isomerization kinetics is important since they represent crucial components for the development of functional photoresponsive materials,[3,6−9] light-powered molecular machines,[10−15] and in photopharmacology,[16,17] where spatiotemporal control of molecular transitions/reactions is needed. In nature, a widely employed strategy for controlling chemical reactions involves accommodating the reactants in a confined space, where encapsulation may influence and control reaction mechanism and kinetics. Enzymes, for example, can catalyze and control reactions with exquisite efficiency and fidelity by exploiting principles of molecular confinement and selective molecular/supramolecular host−guest interactions.[18−21]

In the attempt to mimic natural catalytic systems, chemists have designed synthetic cavities that exploit specific and nonspecific interactions to accommodate reactants with high selectivity in a confined space.[22] Notable examples of synthetic confined spaces are nanopores within metal−organic frameworks,[23−25] surfaces of nanoparticles[26−28] and nanopores within their aggregates,[29] microemulsion droplets,[30,31] and cavities within molecular capsules.[32] Alternatively, cavities can be found within self-assembled cages[33−38] that can encapsulate reactants in solution.[39,40] Confinement inside such cavities has been shown to be crucial in accelerating chemical reactions[29,41−43] or stabilizing otherwise unstable species.[44−48] Notable studies have reported that the photoisomerization of molecular switches can be accelerated,[49] slowed down,[50] or even completely inhibited within crowded molecular environments.[51,52] In some cases, the isomerization of photoresponsive guests may also result in expulsion of the guest[53,54] and even in disassembly of the cage.[55] A key role is attributed to the structural rigidity of synthetic host cavities, which are not capable of accommodating the large conformational changes associated with the photoisomerization of the guest.[1,3,56,57] For this reason, much interest has recently been directed toward the design of flexible molecular cages.[58−61]

In this sense, an interesting example is self-assembled metal−organic cage shown in Figure 1A.[61] This cage has been observed to encapsulate and allow for water solubilization of several different molecular switches, including azobenzene (AZB), methoxylated azobenzene (M-AZB), fluorinated azobenzene (F-AZB), various spiropyrans, as well as

Received: March 29, 2020
Published: April 30, 2020

Downloaded via giovanni m. pavan on November 23, 2020 at 13:57:43 (UTC).
See https://pubs.acs.org/sharingguidelines for options on how to legitimately share published articles.

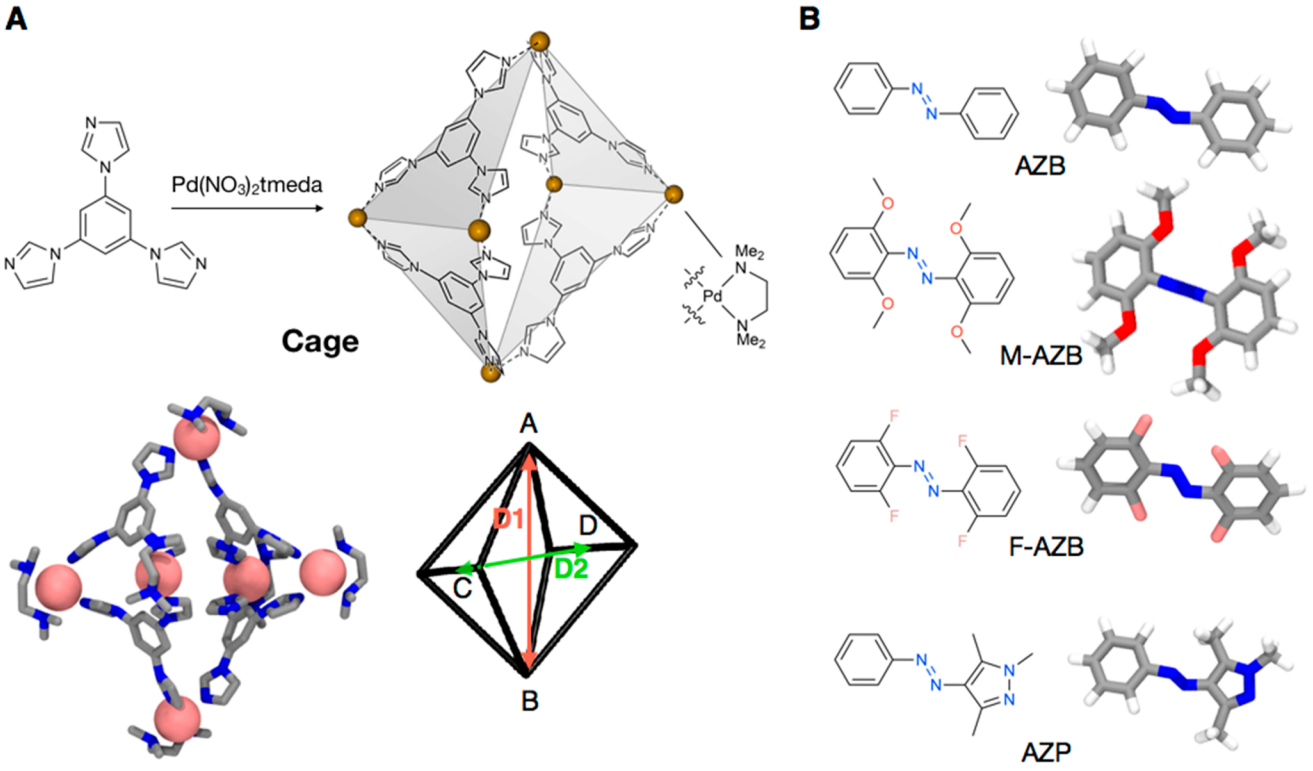

Figure 1. Model host–guest systems. (A, top) Structure of the supramolecular cage studied herein, formed via the self-assembly of triimidazole-based donors and *cis*-blocked Pd acceptors. (A, bottom) Atomistic model of the supramolecular host cage, along with a schematic representation of its octahedral structure, which can be described by the axial and equatorial distances, *D1* (red) and *D2* (green). (B) Structural formulas and atomistic models of the guests studied herein: azobenzene (AZB), methoxylated azobenzene (M-AZB), fluorinated azobenzene (F-AZB), and arylazopyrazole (AZP) (here shown as *trans* isomers).

arylazopyrazole (AZP) (Figure 1B).[62−64] NMR and UV/vis absorption studies provided useful information about the guest encapsulation and the host–guest stoichiometry in these systems.[62−64] X-ray crystallography provided additional experimental insight on the conformations of the crystallized complexes.[62,64] Qualitatively, these efforts indicated that encapsulation and switching of the guests are enabled by large distortions within the cage structure, while confinement alters the isomerization behavior of the guests.[63]

These findings suggest that the flexibility of the cage enables adaptation of its cavity in response to the isomerization of encapsulated guests. However, a clear understanding of the flexibility exhibited by such cages in solution is difficult to obtain experimentally. In particular, correlating such effects with isomerization events that occur on very fast time scales[52] (the *trans* → *cis* isomerization of excited azobenzene occurs on the order of picoseconds in the absence of confinement) and studying the mechanisms that control photoswitching under confinement are prohibitive tasks. In these cases, however, molecular simulations are extremely useful. Quantum mechanics/molecular mechanics (QM/MM), all-atom (AA), and coarse-grained (CG) simulations have been used to investigate azobenzenes and their isomerization within dense monolayers, nanocavities, supramolecular tubules, nanoparticles, and vesicles,[6,8,29,49,50,52,65−68] to name a few. Molecular models can provide detailed insight on the isomerization process[49,52] as well as on the effect of these molecular transitions on the stability[8,66,69] and out-of-equilibrium behavior of the system.[50]

Here we used AA molecular simulations to obtain an exhaustive characterization of the host–guest systems involving azo compounds AZB, M-AZB, F-AZB, and AZP (Figure 1B) as the guests and cage shown in Figure 1A as the host. Combining molecular dynamics (MD) and metadynamics (MetaD) simulations, our approach allows a thorough exploration of the flexibility of the cage in solution and of the mechanisms of guest encapsulation and release under realistic conditions. Coupled with a kinetic study of the isomerization of the excited guests within the cage, these simulations allow us to reconstruct the role of confinement on guest switching and to study the molecular factors that may allow control over this process. We found structure–reactivity relationships having a general character, which may have a profound impact on the rational design of molecular systems with programmable photoswitching properties.

RESULTS AND DISCUSSION

Characterization of Cage Flexibility in Solution. The first step to understanding the behavior of the system is to determine the most favorable conformation(s) assumed by the cage, and how flexible this is in solution under realistic conditions (solvent, temperature, etc.). We started by considering the native cage, without incorporated guests. We developed an atomistic model of the cage (Figure 1A, bottom), starting from the crystal structure for the same cage containing two *trans*-F-AZB guests (which have been manually deleted).[62] Starting from this extended conformation of the cage, we ran a classical MD simulation in explicit water molecules at 297 K and 1 atm (see SI Methods section for details). During this MD run, we analyzed the structural rearrangements of the cage by monitoring two variables describing the geometry of the

https://dx.doi.org/10.1021/jacs.0c03444
J. Am. Chem. Soc. 2020, 142, 9792−9802

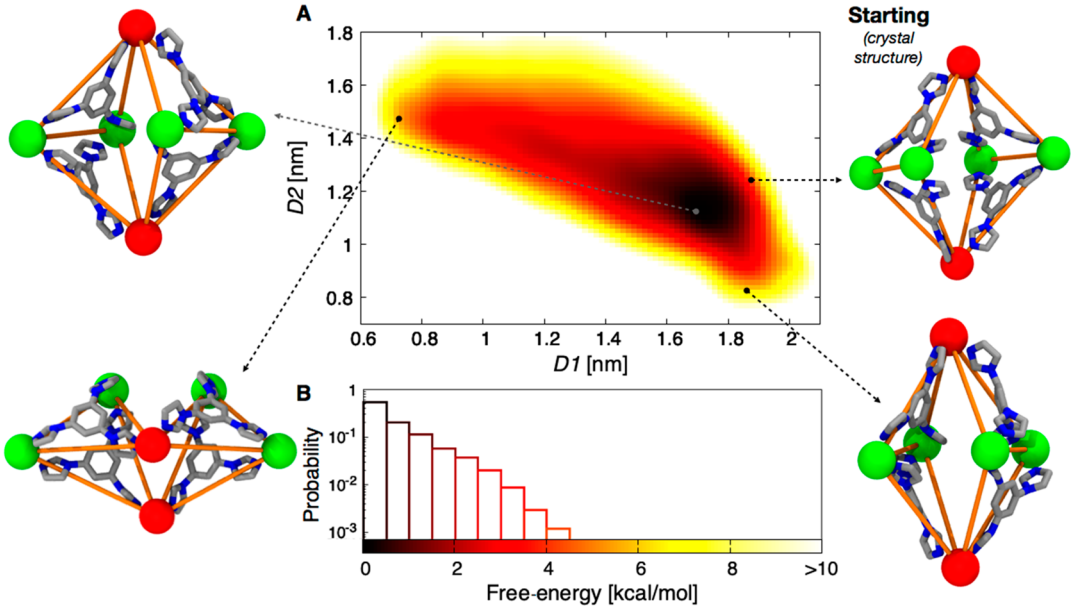

Figure 2. Conformational free-energy landscape of the empty cage. (A) Free-energy surface (FES) as a function of *D1* (distance between the axial/red Pd atoms) and *D2* (distance between the midpoints of opposite edges of the cage identified by the equatorial/green Pd atoms). The color scale in the FES indicates the free-energy associated with cage conformations on the *D1*–*D2* plane (scale and legend shown in B). Four representative snapshots are shown: the starting, extended configuration (top right) corresponding to the crystal structure of the cage,[62] the energetic minimum of the FES (top left), a *D1*-elongated structure (bottom right), and a *D2*-elongated structure (bottom left). Axial and equatorial Pd atoms are colored in red and green, respectively, while the connectivity scheme is colored in orange to facilitate interpretation of the structures. (B) Probability associated with all cage conformations as a function of the relative free-energy (bin width, 0.5 kcal/mol).

cage: *D1*, the axial distance between the "top" and "bottom" Pd atoms (Figure 1A, bottom; points A and B), and *D2*, the distance between the midpoints of the two opposite equatorial edges of the octahedral cage (points C and D). In agreement with previous studies,[63] this preliminary MD simulation showed a significant flexibility within the cage. As seen in Figure S1, *D1* and *D2* have been found to undergo large structural fluctuations, which, however, are observed rarely during 1 μs of a MD simulation.

To better characterize the conformational landscape and the slow structural dynamics of the cage, we turned to MetaD,[70] which allows a more exhaustive exploration of the conformational space of the cage in solution. Using the same operative conditions, we ran a MetaD simulation exploring the possible structural conformations that the cage can dynamically assume in the solvent. In the MetaD run, we used *D1* and *D2* as the collective variables, descriptors of the cage conformations (see SI Methods for details). From this simulation, we could reconstruct the free-energy surface (FES) for the system as a function of *D1* and *D2*. Shown in Figure 2, the FES shows the conformational landscape of the cage (i.e., all the possible conformations that the cage can assume) associated with its relative free-energy. Dark regions in the FES identify the minimum energy (most favorable) configurations for the cage, while red, orange, yellow regions identify conformations that are increasingly higher in free-energy. We can observe a single free-energy minimum (the black region in figure) in which the cage is mildly elongated along the *D1* axis (top left snapshot in Figure 2), and is generally less extended than the initial crystal structure for the cage, which is found ∼4−5 kcal/mol higher in free-energy (Figure 2, top right snapshot). Exploiting the rotation of the 12 imidazole-rings with respect to the central benzene ring,[62] the MetaD allows the system to explore a wide range of conformations (including very elongated shapes), a selection of which are shown in Figure 2. In most cases, these configurations are considerably higher in free-energy and are thus unlikely to be observed in solution. Furthermore, we calculated the probability associated with the different colored regions of the FES (see SI Methods). The result of this analysis (Figure 2B) shows that, from a statistical point of view, only the cage configurations lying within 1.5 kcal/mol of the global minimum are really accessible by the cage (dark regions on the FES and first three bins of Figure 2B). This means that the cage will most likely assume configurations within *D1* ∼ 1.4−1.9 nm and *D2* ∼ 0.9−1.3 nm (dark FES region). Under these conditions, these conformations will constitute ∼90% of the global population of cages in the system. It is worth adding that the shape of the FES minimum also provides important information about the flexibility of the cage in solution. In this case, the FES minimum is quite broad, which is in agreement with the experimentally observed[63] high flexibility of the cage. Altogether, this analysis provides interesting information not only on the level of flexibility of the cage under experimentally relevant conditions, but also on what we could reasonably/statistically expect to find in terms of the structural diversity of the cage in a realistic solution.

Effects of Guest Encapsulation on Cage Flexibility. The flexibility of the cage influences its ability to encapsulate guest molecules. Conversely, guest encapsulation itself may have an effect on the flexibility of the cage. For our next step, we thus studied the effect of guest encapsulation on the cage. Starting again from the crystal structure of the cage containing two *trans*-F-AZB guests,[62] we deleted one guest and replaced the remaining one, where necessary, in order to obtain starting models for the cage encapsulating one F-AZB, M-AZB, AZP, or AZB guest (Figure 1B). These starting host−guest complex models were then equilibrated via 1 μs of MD simulation (see SI Methods for details). In particular, we compared the effect

https://dx.doi.org/10.1021/jacs.0c03444
J. Am. Chem. Soc. 2020, 142, 9792−9802

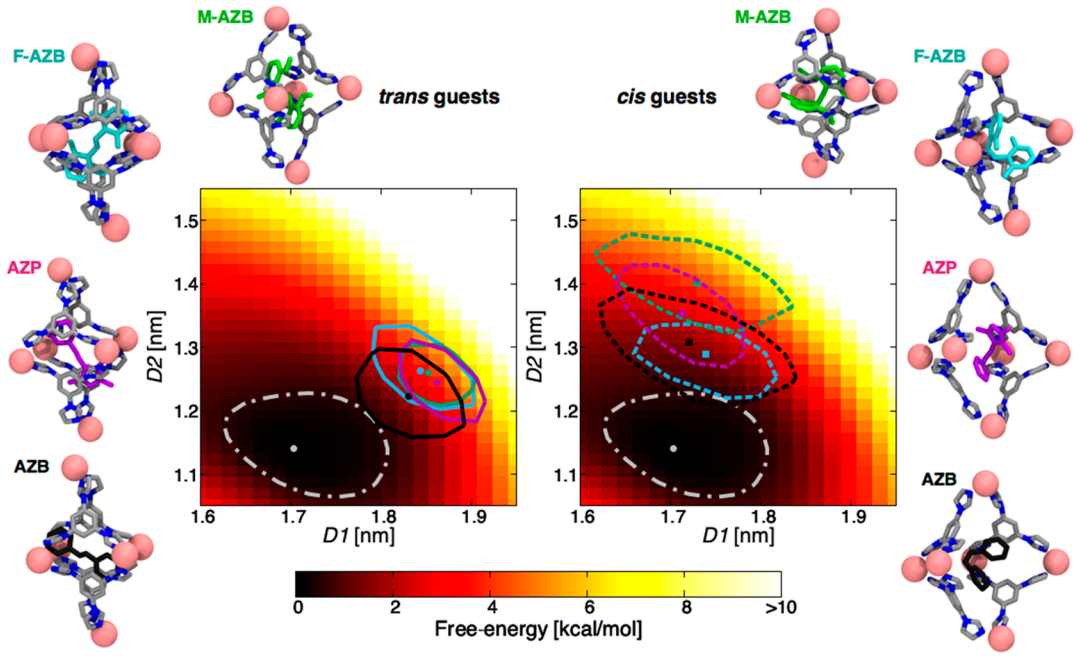

Figure 3. Free-energy cost of guest encapsulation. Representative equilibrium conformations (in the *D1*−*D2* plane) of the cage encapsulating different *trans* (left) or *cis* (right) guests. For each host−guest system, we report the position of the minimum-energy conformation (colored points) and the associated isolines (same colors) enclosing all conformations within 0.5 kcal/mol from the minimum of each system. The data are projected onto the FES of the empty cage (same as Figure 2), for which we also indicate the global minimum and associated 0.5 kcal/mol isoline (in white).

of incorporating either *trans* or *cis* conformers of all guests, analogous to the states of the cage before and after the isomerization. In all cases, we monitored the equilibrium conformations of the cage in terms of *D1* and *D2*. We could observe that all guests remained steadily bound within the cage during the whole MD simulation time. Figure 3 shows the equilibrium configuration for the cage in terms of *D1* and *D2* in all cases (colored points) on the FES of the empty cage. The colored isolines in Figure 3 identify the associated free-energy regions within 0.5 kcal/mol of the global minima for each case (the same isoline for the empty cage is shown in white).

On the basis of the data in Figure 3, we can draw the following conclusions. In order to incorporate a guest, the cage must undergo structural rearrangements, specifically to open up, which is accompanied by a free-energy cost. The FES data in Figure 3 allows us to assess the free-energy penalty associated with encapsulation of each guest. This value can be calculated as the difference in free-energy between the white point (empty cage) and the colored points (a higher free-energy configuration that the cage has to reach to encapsulate the guest). We have found values for ΔG in the range ∼3−5 kcal/mol, depending on the guest. Such a free-energy penalty can be seen as an entropic cost (i.e., unfavorable) for the encapsulation, as the cage elongates both axially and equatorially upon encapsulating the guest. From the data in Figure 3 we can also observe how guest encapsulation affects the flexibility of the cage. In general, the colored isolines encompass a smaller area than the white isoline associated with the empty cage. This observation suggests that the cage loses flexibility upon encapsulating a guest, the effect being more pronounced for *trans* (left panel) than for *cis* guests (right panel). Moreover, by comparing the regions occupied by the cage when hosting *trans* or *cis* guests, we note that they enclose similar free-energy values. This result suggests that isomerization of the encapsulated guest would not require a consistent free-energy cost in terms of host deformation, thus demonstrating the energetic accessibility of the process. These results are consistent with the evidence that the *trans* → *cis* isomerization of the guests occurs inside the cage, and the resulting *cis* complexes remain stable also after isomerization.[62−64]

Experiments have shown that our cage can often accommodate two *trans* guest molecules at the same time.[62,64] On the basis of these observations, we have modeled two additional systems wherein the cage encapsulates two *trans*-AZBs or two *trans*-F-AZBs, and have obtained equilibrated configurations for these complexes via 1 μs of MD simulation. In these cases, we observed that the cage undergoes considerable deformations compared to when only one encapsulated *trans* guest is present in the cavity of the model cage (see Figure S2). However, the stability observed for two-guest complexes suggests that the affinity between the encapsulated guests and the cage is significant. We anticipate that this competition between the free-energy penalty associated with the crowding inside the cage cavity and the host−guest affinity represents a crucial factor that can regulate the reactivity of these host−guest complexes.

***Trans*−*Cis* Isomerization of Azobenzenes Inside the Cage.** An interesting question is how, and to what extent, the switching of excited azobenzenes is affected by encapsulation inside the cage. The *trans* → *cis* isomerization of azobenzenes occurs mainly via a rotational mechanism involving the torsion of the central N−N bond, which produces the out-of-plane rotation of one end of the molecule[71,72] (see snapshots in Figure 4A). To simulate the *trans* → *cis* transition of the guests within the cage, we use a model for excited *trans*-azobenzenes (*S**) that has been recently employed to study azobenzene switching inside self-assembled tubules via atomistic and

https://dx.doi.org/10.1021/jacs.0c03444
J. Am. Chem. Soc. 2020, 142, 9792−9802

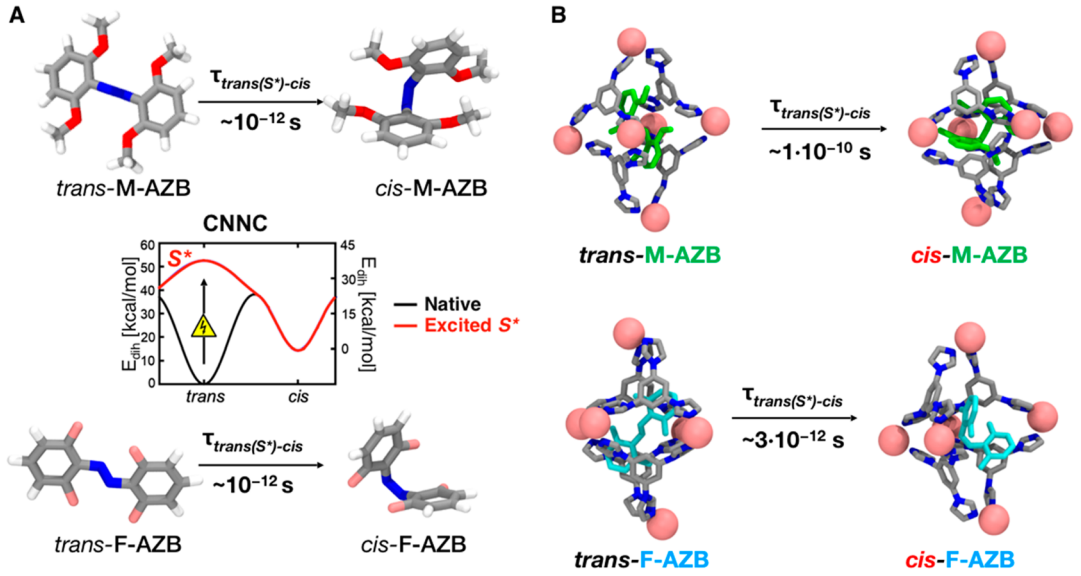

Figure 4. *Trans* → *cis* transitions of azo-switches inside and outside the cage. (A) Kinetics of *trans* → *cis* isomerization of the excited M-AZB (top) and F-AZB (bottom) outside the cage (in solution) reported as examples. The measured transition times, reported below the isomerization arrows, are obtained from MD simulations using an atomistic model where the CNNC dihedral potential term for the *trans*-azobenzene derivatives (E_{dih}, reported in the plot as a function of the dihedral angle), is changed from the black curve (native/unperturbed state) to the blue curve (excited *trans*-azobenzene, *S**).[50] (B) Kinetics of *trans* → *cis* isomerization of excited M-AZB (top) and F-AZB (bottom) switches confined inside the cage. Transition times for all the guests in the cage are reported in Table 1.

Table 1. Thermodynamic and Kinetic Data for *trans* Guest Binding and Isomerization Inside the Cage

guest	ΔG [kcal/mol]	τ_{off} [s]	K_b [M^{-1}]	k_{off} [s^{-1}]	k_{on}[a] [M^{-1} s^{-1}]	$\tau_{trans-cis}$ [s]
AZB	−5.3 ± 0.3	(3.9 ± 0.2) × 10^{-4}	7.87 × 10^3	2.65 × 10^3	2.1 × 10^7	(1.05 ± 0.05) × 10^{-12}
M-AZB	−7.9 ± 1.3	(1.2 ± 0.1) × 10^{-2}	6.41 × 10^5	8.3 × 10^1	5.32 × 10^7	(1.00 ± 0.05) × 10^{-10}
F-AZB	−5.3 ± 0.9	(3.8 ± 0.1) × 10^{-3}	7.87 × 10^3	2.63 × 10^2	2.1 × 10^6	(3.0 ± 0.1) × 10^{-12}
AZP	−5.7 ± 0.8	(4.2 ± 0.1) × 10^{-4}	1.55 × 10^4	2.38 × 10^3	3.7 × 10^7	(1.25 ± 0.05) × 10^{-12}

[a]Guest concentration in the model systems is ∼11.4 mM; to obtain the effective k_{on} values in [s^{-1}], the values in the table should be multiplied by 11.4 mM.

coarse-grained simulations.[50] In this atomistic model, the central CNNC dihedral potential term for the azobenzene unit is modified from the black curve (unperturbed *trans*-azobenzene) into the blue curve in the inset of Figure 4. In this model, the *trans*-azobenzene guest, which is assumed to reach the excited state (*S**), undergoes spontaneous *trans* → *cis* switching according to the correct transition pathway and kinetics during classical MD runs.[50] Starting from the equilibrated models for the cage encapsulating single molecules of each *trans* guest (Figure 3, left), we studied the kinetics of their switching inside and outside the cage by means of MD simulations.

As shown in Figure 4A, the isomerization of all excited unbound *trans*-azobenzenes studied here occurs on the time scale of picoseconds, consistent with the kinetics of isomerization for free azobenzenes (unconstrained conditions).[52] However, the process can become significantly slower as a result of encapsulation within the cage (see Figure 4B) (i.e., molecular crowding).[50] The *trans* → *cis* isomerization times for the guests studied herein are reported in Table 1. Interestingly, the slowing of the transition can be negligible or different by of orders of magnitude, depending on the encapsulated guest. For example, in the case of AZB and AZP, the transition kinetics is not significantly affected by the confinement in the cage. On the other hand, the switching is ∼3 or even up to ∼100 times slower for confined F-AZB and M-AZB, respectively (Figure 4B). Moreover, it is worth noting that such a considerable switching deceleration is obtained using a model where the excited *trans* guests cannot de-excite back.[50] Considering that the lifetime of the excited state *S** of *trans*-azobenzene is on the order of picoseconds,[52] however, de-excitation of *S** to the ground state is a non-negligible event in real systems. This suggests that the considerable deceleration in transition rates associated with encapsulated F-AZB and M-AZB could actually be, at worst, underestimated by our model. Such a difference is interesting, especially considering that cases have been reported in which azobenzene isomerization may become rare (as in highly ordered self-assembled tubules[50]) or impossible (such as within dense azobiphenyl monolayers[52]).

In our specific systems, guest isomerization may even result in an unstable complex. This is the case when the cage incorporates two *trans*-F-AZB guests at the same time. Right after isomerization is triggered in this system, one of the two encapsulated guests is expelled from the cage.[62] Interestingly, we found the same behavior in our simulations (Figure S3). Co-encapsulation of one *trans*- and one *cis*-F-AZB guest inside the cage leads to a highly unstable species, leading to the release of one of the two guests within short time scales (∼10−100 ns). The molecular factors that may affect the switching process inside the cage cavity will be discussed more in detail in the last section. Nonetheless, these results indicate that in order to fully understand and characterize the transitions in

https://dx.doi.org/10.1021/jacs.0c03444
J. Am. Chem. Soc. 2020, 142, 9792−9802

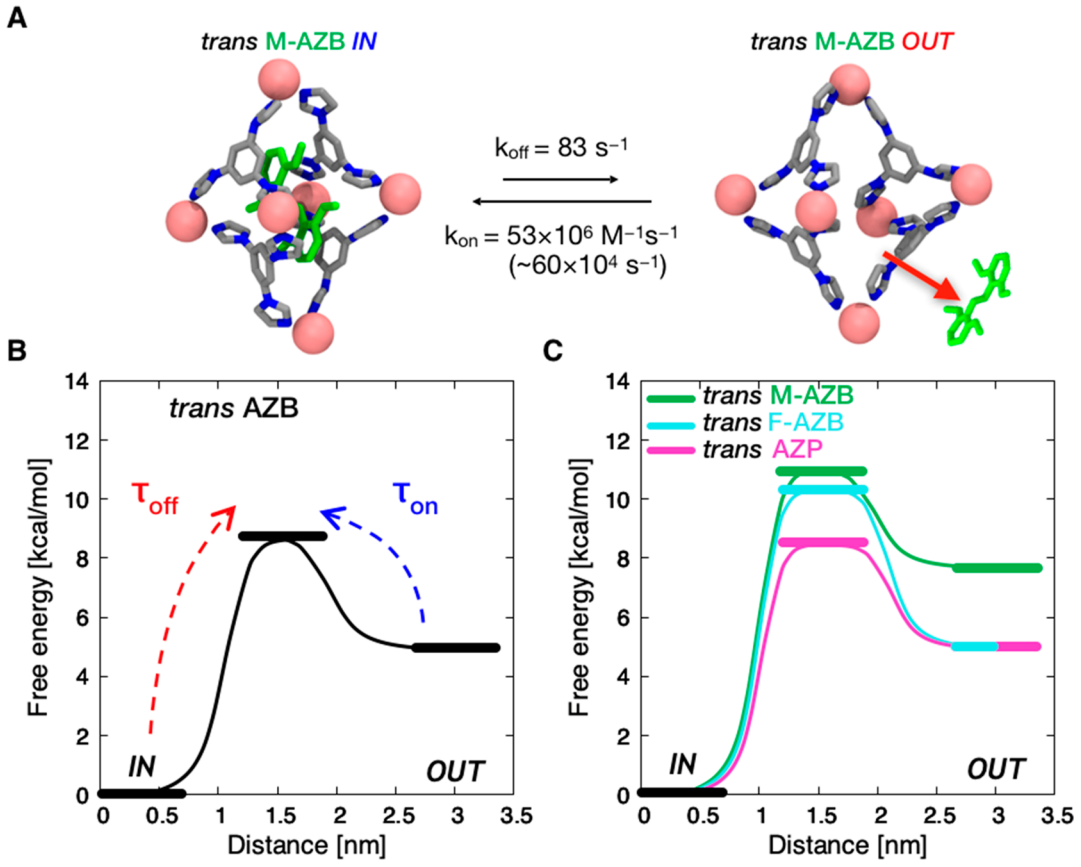

Figure 5. Thermodynamics and kinetics of *trans* guest binding/release. (A) Representative MetaD snapshots of the reversible binding and release of *trans*-M-AZB inside the cage; k_{off} and k_{on} denote the kinetic constants for the expulsion and encapsulation processes (the k_{on} value inside the brackets is explicitly calculated, accounting for the guest concentration used in the model ~11.4 mM, providing the actual rate). (B) Thermodynamic and kinetic scheme representing the expulsion and encapsulation mechanisms for *trans*-AZB in/out the cage as a function of the distance between the guests' and the cage's centers of mass (identifying IN and OUT states). (C) Thermodynamic schemes representing the expulsion/encapsulation of the *trans* isomers of M-AZB (green), F-AZB (cyan), and AZP (violet) guests. All ΔG differences between IN vs OUT states were computed from converged MetaD simulations, while the transition barriers were more accurately estimated from multiple infrequent MetaD runs (see the SI Methods section for further details).

these systems, it is first necessary to study the intrinsic dynamics of the host−guest complexes and the kinetics of guest encapsulation and release.

Mechanisms of Guest Encapsulation/Release and Switching. The results discussed in the previous section provide information about the kinetics of *trans* → *cis* switching of excited guests inside the cage. However, this information is not sufficient to draw conclusions about whether the isomerization occurs inside or outside the cage, or about the stability of the guest encapsulation inside the host before and after the transition. To obtain a complete picture of the transition mechanism, we have studied the thermodynamics and kinetics of the guest encapsulation and expulsion in/out the cage. In fact, the ΔG for guest encapsulation (and the related k_{on} vs k_{off}) determines the effective probability of finding the guests inside/outside the cage and their residence time inside the cage.

Since guest encapsulation and release are, in general, rare events in these systems, it is difficult to study them via classical MD simulations. Consequently, we used MetaD simulations to investigate the thermodynamics and kinetics of guest binding/release. Starting from the equilibrated *trans* complexes, we conducted MetaD simulations during which the guests exchange multiple times in and out of the cage, allowing for a thorough exploration of the bound and unbound states and of the transition between them. These simulations allowed us to retrieve the free-energy difference, ΔG, between the encapsulated and free states and to calculate the corresponding K_b values (see Figure 5 and Table 1 for the data for all *trans* guests; the complete series including *cis* guests is listed in Tables S1 and S2). These data offer an exhaustive picture of the thermodynamics governing guest encapsulation, which is crucial to uncovering the probability of guest binding/release. We found that formation of the host−guest complex is energetically favored in all the tested cases, with a free-energy gain ranging from ~3.6 kcal/mol for *cis*-F-AZB up to ~8 kcal/mol for *trans*-M-AZB.

As recently done to study the kinetics of monomer exchange in supramolecular polymers,[73] we then studied the kinetics of guest binding/release by means of infrequent MetaD simulations[74] (see SI Methods for details). From multiple infrequent MetaD runs activating/biasing guest release out from the cage, we could reconstruct unbiased kinetics for the event and estimate residence times for the encapsulated guest, τ_{off}. The kinetic constant for guest release can be calculated as $k_{off} = 1/\tau_{off}$. The kinetic constant for guest encapsulation (k_{on}) can be then derived as follows: $K_b = k_{on}/k_{off}$. In this way we can obtain the complete thermodynamic and dynamic character-

https://dx.doi.org/10.1021/jacs.0c03444
J. Am. Chem. Soc. 2020, 142, 9792−9802

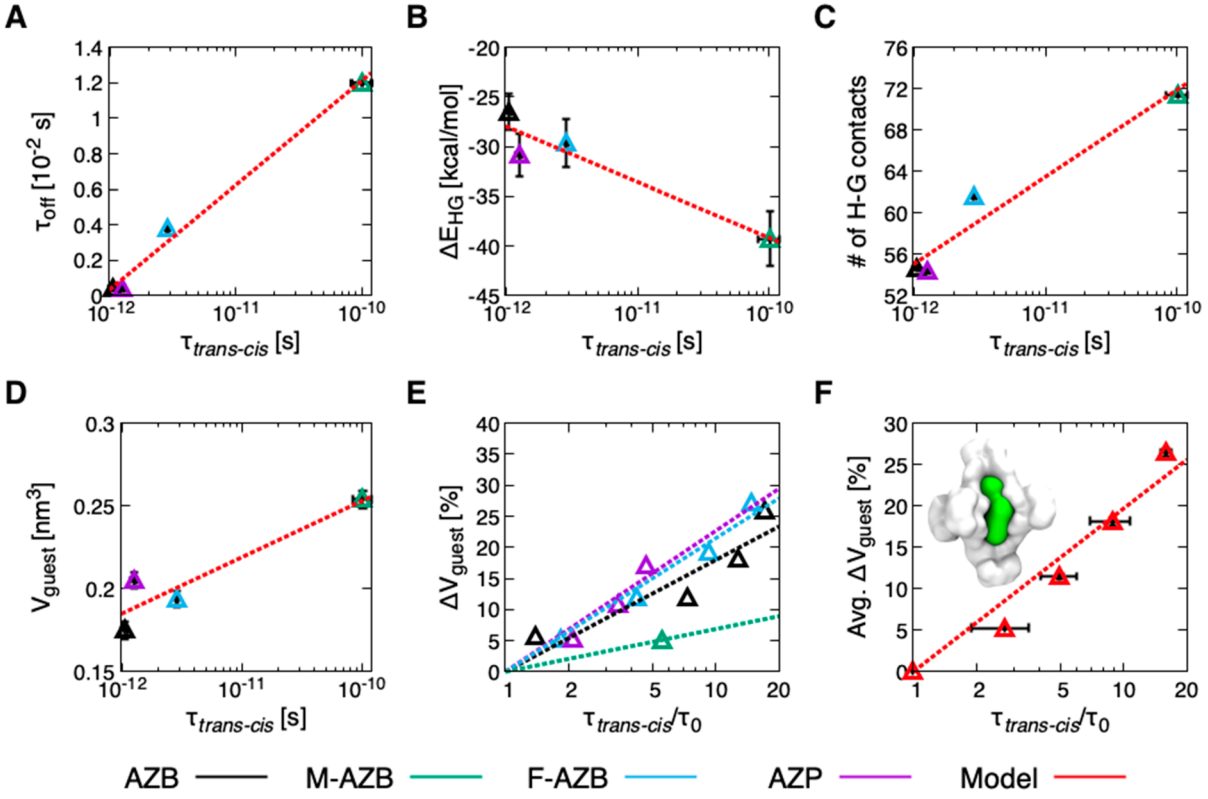

Figure 6. Molecular determinants of isomerization under confinement. (A) Relationship between isomerization rate ($\tau_{trans-cis}$) and residence times (τ_{off}) of the guests inside the cage. (B) Relationship between $\tau_{trans-cis}$ and potential energy of host−guest interactions, ΔE_{HG}. (C) Relationship between $\tau_{trans-cis}$ and the number of contacts between the cage and the guest. (D) Relationship between $\tau_{trans-cis}$ and the volume (V) of guest molecules (see the SI Methods section for details on guest volume estimation). (E) Switching deceleration, $\tau_{trans-cis}/\tau_0$, as a function of the increase in guest volume ($\%\Delta V_{guest}$), in which τ_0 denotes isomerization time measured at the original volume of each guest. In plots A−E, the points correspond to guests AZB (black), M-AZB (green), F-AZB (cyan), and AZP (violet). (F) Average $\tau_{trans-cis}/\tau_0$ as a function of the average increase in guest volume ($\%\Delta V_{guest}$), obtained by averaging all data from plot E between systems with similar $\%\Delta V_{guest}$. The error bars indicate the standard deviation of $\%\Delta V_{guest}$ and $\tau_{trans-cis}/\tau_0$ values. Inset: cartoon showing the volume of encapsulated M-AZB (green) inside the cage (white). The dashed lines in all plots are the logarithmic fit of the data.

ization of these host−guest systems, as represented in the thermodynamic schemes in Figure 5 and in the data collected in Tables 1, S1, and S2. These results reveal some subtle aspects of the binding/release processes. For example, we found that the *cis* conformers on average exhibit shorter residence times inside the cage with respect to the corresponding *trans* isomers, including more weakly binding *trans* isomers such as *trans*-AZB and *trans*-AZP. This effect is attributed to the lower free-energy barrier that the *cis* guest has to overcome to leave the cage as compared to the *trans* guest (see Table S2), which could be correlated with the relatively high flexibility of the host cage while accommodating *cis* guests (see Figure 3). Most importantly, we can observe from Table 1 that the characteristic transition times for *trans* → *cis* isomerization ($\tau_{trans-cis}$) are orders of magnitude shorter than the characteristic time for the release of *trans* guests from the cage (τ_{off}). This indicates that isomerization in these systems occurs most probably inside the cage.

We also conducted MetaD simulations to study the encapsulation of a second *trans* guest in the case where one *trans* guest is already encapsulated inside the cage. We know from the experimental results[62] and from the plain MD simulations (see previous sections), that the cage can often incorporate two *trans* guests (e.g., F-AZB or AZB). Conversely, other molecules, such as M-AZB, can only form complexes incorporating one guest molecule.[62] The FESs obtained from MetaD simulations with two M-AZB vs two F-AZB or two AZB guests are consistent with this picture (Figure S4). In particular, these results clearly demonstrate that while incorporation of a second F-AZB, or AZB, guest in the cage is an energetically favored event (Figure S4, center and right), in the case of M-AZB, this process is highly unfavorable and unlikely (Figure S4, left). This is consistent, for example, with the available crystal structures, showing that two *trans*-F-AZB and two *trans*-AZB guests can be encapsulated within one cage, while the same cage accommodates only one *trans*-M-AZB at a time.[62] Moreover, while quantities such as the ΔG, K_b, k_{on}, and k_{off} of guest encapsulation/expulsion can be difficult to determine experimentally, the overall binding constant governing encapsulation of two *trans*-AZB guests within the cage could be estimated from NMR experiments, giving a value in the range of $\sim 10^9$ M^{-2}.[62] We could also estimate such overall binding constant (K_b(tot)) from the MetaD simulations using the K_b values associated with the first and the second *trans*-AZB guests (i.e., as K_b(tot) = K_b(guest-1) × K_b(guest-2)). The calculated value for K_b(tot) is $\sim 0.3 \times 10^9$ M^{-2} (see Table S3), which is consistent with the value obtained experimentally. The results of our simulations are also qualitatively consistent with the experimental evidence available for the other systems, for which experimental K_b values could not be obtained. We conducted infrequent MetaD simulations to compare the residence times of two F-AZB

https://dx.doi.org/10.1021/jacs.0c03444
J. Am. Chem. Soc. 2020, 142, 9792−9802

guests inside the cage before and after *trans* → *cis* isomerization of one guest. We found that while the switching similarly occurs within the cage, one of the two guests is then expelled promptly, within very fast time scales (nanoseconds)—orders of magnitude shorter than in the two-*trans* case (see Figure S3). In particular, the expulsion of *cis*-F-AZB is ten times more likely (or faster) than that of the *trans* isomer (residence times inside the cage of ∼10 ns and ∼100 ns, respectively; see also Figure S5). This finding is consistent with the experimental results[62] demonstrating that the (*trans*+*cis*)-cage ternary complex is unstable and that the isomerization of *trans*-F-AZB produced the rapid expulsion from the cage of one out of the two guests (most likely the *cis* isomer). Together, these results support the reliability of our models and provide a comprehensive characterization of the system both from thermodynamic and kinetic points of view. They also show how, in order to characterize the transition kinetics inside the cage, it is also necessary to characterize the binding and release of the guests in/out the cage.

Molecular Determinants of Guest Transitions in the Cage. In the final step, we analyzed the results from our simulations to investigate the molecular determinants that control in-cavity isomerization of the guests in these systems. Table 1 lists data describing dynamic host−guest binding in the systems and the kinetics of isomerization inside the cage cavity. Interestingly, by comparing the $\tau_{trans-cis}$ with the τ_{off} data, we obtain a nontrivial relationship between the residence time of the guests inside the host and the characteristic time scale needed for guest switching. In particular, we can observe that longer residence times in the cavity correspond to slower transitions (Figure 6A), suggesting that the same molecular factors regulating the stability of host−guest binding have an impact on the switching rates of the guests.

In general, the energy of the host−guest interaction ΔE_{HG} correlates with τ_{off}. When this interaction is stronger, guest release from the cage is slower, meaning that the guest spends more time in the cage. Molecular crowding in the cavity has a similar effect. When there is a higher number of contacts between the host and the guest, τ_{off} is longer, and guest release is less probable. We can clearly observe this effect for all simulated systems, both with *trans* and *cis* guests (see Figure S6A,B). This result is reasonable, as the interactions and the number of contacts between the host and the guest are intimately correlated to one another (see Figure S6C). This correlation is especially relevant when considering flexible hosts: stronger affinity between the host and guest leads to larger deformation of the host, as a flexible cage can structurally adapt to enhance contacts with the guest. At the same time, the relationship obtained in Figure 6A indicates that both host−guest affinity and molecular crowding impact the transition rate ($\tau_{trans-cis}$). This relationship between $\tau_{trans-cis}$ and ΔE_{HG}, and between $\tau_{trans-cis}$ and the number of contacts, is demonstrated by the trends in Figure 6B and C, respectively. These results suggest that both host−guest affinity and molecular crowding can in principle be used to control the transition rates in the system.

Because extrapolating design principles from these plots is not trivial, we chose a more elegant strategy. We started from the simplistic consideration that, for a given impact of host−guest contacts on the switching process, the ratio between the volume occupied by the guest and the volume accessible in the cage (e.g., V_{guest}/V_{cavity}) constitutes a discriminant parameter governing transitions in the system. Given that the cage is the same in all systems, and assuming that the variations in V_{cavity} are negligible when comparing between the various systems (simplification), we plotted V_{guest} against $\tau_{trans-cis}$ (Figure 6D) and obtained a trend similar to those described above. Even considering the approximations required to make this observation, this qualitative trend reveals a molecular-level relationship between the volume of the guest and the transition rate under confinement.

Recently, we demonstrated how reliable chemically relevant molecular models can be used as "toy models" to obtain pseudomolecular, yet useful information. By "playing" with these flexible models, we can then learn about the factors that control the system.[50,73] Having observed that guest volume has a strong impact on transition rate within the cage, we developed a computational strategy to increase the number of available data points in this trend. Starting from equilibrated models of the cage encapsulating one *trans* guest of each type, we artificially increased the radii of guests' atoms in the models to increase V_{guest}. In all cases, the atomic radii have been increased to achieve a global increase of ∼5, 10, 20, or 30% for V_{guest}. Repeating the isomerization simulations for all these cases then allowed us to monitor transition deceleration as a function of the increase in guest volume ($\%\Delta V_{guest}$). In this way, we obtained the trends shown in Figure 6E for the various guests.

These results show that transition rate generally slows down as $\%\Delta V_{guest}$ increases. Some variability between the different guests can be expected (e.g., M-AZB in green), as other features of the guest, such as chemical structure and shape, can also impact isomerization. These results are in agreement with our observation that host−guest affinity also has an impact on the rate of isomerization (Figure 6B). We also note that for some guests (M-AZB and AZP), the series is incomplete because isomerization does not occur inside the cage over a certain $\%\Delta V_{guest}$ (∼20% for AZP and ∼5−10% for M-AZB). In these cases, isomerization is either impeded by the cage or results in the release of the isomerizing guest. This observation is consistent with experimental results and with the simulations for two-guest systems. In fact, encapsulating two guests inside the cage can be assumed to be comparable to a $\%\Delta V_{guest}$ of ∼100%, well over the maximum $\%\Delta V_{guest}$ for which isomerization occurs inside the cage. As previously shown, isomerization of one guest produces rapid expulsion of one guest from two-guest systems (see Figure S3).

Finally, if we average the rate deceleration data at different values of $\%\Delta V_{guest}$ for the various systems (Figure 6E), we obtain the plot shown in Figure 6F, which shows a clear general trend between the average increase in guest volume and the deceleration of guest transitions. This trend is clearly qualitative, as other variables may also be important in controlling guest isomerization under confinement. Nevertheless, this result demonstrates a direct correlation between guest volume, crowding within the cage, and the guest transition rates. This observation helps rationalize experimental[62,75] and computational results,[50,52,76] showing that azobenzene isomerization may be hindered in highly crowded molecular systems. The generality of the computational approach presented herein offers a context for developing the idea that molecular environments can be, in principle, rationally designed to control molecular switching processes.

https://dx.doi.org/10.1021/jacs.0c03444
J. Am. Chem. Soc. 2020, 142, 9792−9802

CONCLUSIONS

Learning how to control chemical reactions inside confined spaces will unlock many applications. Here we used atomistic simulations to investigate the mechanisms and molecular factors that control *trans* → *cis* isomerization of various azo compounds within a coordination cage. Classical molecular dynamics and metadynamics simulations allowed us to characterize these host−guest systems from thermodynamic and kinetic points of view. In this way, we obtained an exhaustive mechanistic understanding of guest encapsulation, reversible guest uptake/release dynamics and guest switching transitions, and results in agreement with experimental observations.

To elucidate the kinetics of molecular transitions under confinement, we show that it is necessary to understand the intrinsic dynamics of guest binding and release processes. We demonstrate how this equilibrium is influenced by the free-energy cost associated with host reconfiguration upon guest encapsulation, and by the energy gain due to host−guest interactions. This competition determines the residence time of encapsulated azobenzene guests inside the cage and the slowing rate of their isomerization. We identify molecular crowding and host−guest affinity as two key factors governing isomerization rate/probability in these systems. Our results demonstrate that, in principle, tuning the volume of the guest may have a direct impact on the transition rate inside the cage, or even dictate whether the transition will occur inside or outside the cage.

Overall, the advantages of the approach employed herein are many. Our approach enables a thorough characterization of (i) the flexibility and conformations accessible by the cage under given conditions of solvent and temperature, (ii) the isomerization rates for encapsulated guests, and (iii) the effect of guest encapsulation and isomerization on the flexibility and conformational distortion of the cage. The metadynamics simulations allow us to obtain molecular-level information on the thermodynamics and kinetics of the host−guest encapsulation, providing values for, e.g., k_{on}, k_{off}, ΔG, free-energy barriers, etc., which can be challenging to determine experimentally. From a holistic point of view, this reveals the synergies between structure, thermodynamics, and dynamics within these complex molecular systems, which concur to determine the behavior of these host−guest molecular systems. In principle, the molecular simulations approaches described herein are versatile and can be applied to investigate not only other cages but also stimuli-responsive host−guest systems in general. Our approach can provide clearer insight into the molecular factors that control structure, host−guest affinity, and dynamics, thus guiding the rational design, or customization, of systems with controllable reactivity. We envisage that this approach will find application in fields ranging from the rational design of photoresponsive host−guest systems and artificial enzymes to the control of chemical reactions in confined spaces.

ASSOCIATED CONTENT

Supporting Information

The Supporting Information is available free of charge at https://pubs.acs.org/doi/10.1021/jacs.0c03444.

Details on the creation and parametrization of the molecular systems, simulation setup, and analysis of molecular dynamics and metadynamics simulations; additional data and figures from the simulations (PDF)

AUTHOR INFORMATION

Corresponding Author

Giovanni M. Pavan − *Department of Innovative Technologies, University of Applied Sciences and Arts of Southern Switzerland, CH-6928 Manno, Switzerland; Department of Applied Science and Technology, Politecnico di Torino, 10129 Turin, Italy;* orcid.org/0000-0002-3473-8471; Email: giovanni.pavan@polito.it

Authors

Luca Pesce − *Department of Innovative Technologies, University of Applied Sciences and Arts of Southern Switzerland, CH-6928 Manno, Switzerland;* orcid.org/0000-0001-6364-9577

Claudio Perego − *Department of Innovative Technologies, University of Applied Sciences and Arts of Southern Switzerland, CH-6928 Manno, Switzerland;* orcid.org/0000-0001-8885-3080

Angela B. Grommet − *Department of Organic Chemistry, Weizmann Institute of Science, Rehovot 76100, Israel*

Rafal Klajn − *Department of Organic Chemistry, Weizmann Institute of Science, Rehovot 76100, Israel;* orcid.org/0000-0002-6320-8875

Complete contact information is available at: https://pubs.acs.org/10.1021/jacs.0c03444

Notes

The authors declare no competing financial interest.

ACKNOWLEDGMENTS

GMP acknowledges the funding received by the Swiss National Science Foundation (SNSF grant number 200021_175735) and by the European Research Council (ERC) under the European Union's Horizon 2020 research and innovation program (grant agreement no. 818776 − DYNAPOL). The authors also acknowledge the computational resources provided by the Swiss National Supercomputing Center (CSCS). RK acknowledges funding from the Minerva Foundation. ABG acknowledges funding from the Zuckerman STEM Leadership Program.

REFERENCES

(1) Bandara, H. M. D.; Burdette, S. C. Photoisomerization in Different Classes of Azobenzene. *Chem. Soc. Rev.* **2012**, *41*, 1809−1825.

(2) Shi, Z.; Peng, P.; Strohecker, D.; Liao, Y. Long-Lived Photoacid Based upon a Photochromic Reaction. *J. Am. Chem. Soc.* **2011**, *133*, 14699−14703.

(3) Klajn, R. Spiropyran-Based Dynamic Materials. *Chem. Soc. Rev.* **2014**, *43*, 148−184.

(4) Weston, C. E.; Richardson, R. D.; Haycock, P. R.; White, A. J. P.; Fuchter, M. J. Arylazopyrazoles: Azoheteroarene Photoswitches Offering Quantitative Isomerization and Long Thermal Half-Lives. *J. Am. Chem. Soc.* **2014**, *136*, 11878−11881.

(5) Wang, Y.-T.; Liu, X.-Y.; Cui, G.; Fang, W.-H.; Thiel, W. Photoisomerization of Arylazopyrazole Photoswitches: Stereospecific Excited-State Relaxation. *Angew. Chem., Int. Ed.* **2016**, *55*, 14009−14013.

(6) Fredy, J. W.; Méndez-Ardoy, A.; Kwangmettatam, S.; Bochicchio, D.; Matt, B.; Stuart, M. C. A.; Huskens, J.; Katsonis, N.; Pavan, G. M.; Kudernac, T. Molecular Photoswitches Mediating

the Strain-Driven Disassembly of Supramolecular Tubules. *Proc. Natl. Acad. Sci. U. S. A.* **2017**, *114*, 11850−11855.
(7) Yagai, S.; Iwai, K.; Yamauchi, M.; Karatsu, T.; Kitamura, A.; Uemura, S.; Morimoto, M.; Wang, H.; Würthner, F. Photocontrol Over Self-Assembled Nanostructures of π-π Stacked Dyes Supported by the Parallel Conformer of Diarylethene. *Angew. Chem., Int. Ed.* **2014**, *53*, 2602−2606.
(8) Molla, M. R.; Rangadurai, P.; Antony, L.; Swaminathan, S.; de Pablo, J. J.; Thayumanavan, S. Dynamic Actuation of Glassy Polymersomes through Isomerization of a Single Azobenzene Unit at the Block Copolymer Interface. *Nat. Chem.* **2018**, *10*, 659−666.
(9) Pianowski, Z. L. Recent Implementations of Molecular Photoswitches into Smart Materials and Biological Systems. *Chem. - Eur. J.* **2019**, *25*, 5128−5144.
(10) Feringa, B. L. The Art of Building Small: From Molecular Switches to Motors (Nobel Lecture). *Angew. Chem., Int. Ed.* **2017**, *56*, 11060−11078.
(11) Sauvage, J.-P. From Chemical Topology to Molecular Machines (Nobel Lecture). *Angew. Chem., Int. Ed.* **2017**, *56*, 11080−11093.
(12) Stoddart, J. F. Mechanically Interlocked Molecules (MIMs)—Molecular Shuttles, Switches, and Machines (Nobel Lecture). *Angew. Chem., Int. Ed.* **2017**, *56*, 11094−11125.
(13) Dri, C.; Peters, M. V.; Schwarz, J.; Hecht, S.; Grill, L. Spatial Periodicity in Molecular Switching. *Nat. Nanotechnol.* **2008**, *3*, 649−653.
(14) Kassem, S.; Lee, A. T. L.; Leigh, D. A.; Marcos, V.; Palmer, L. I.; Pisano, S. Stereodivergent Synthesis with a Programmable Molecular Machine. *Nature* **2017**, *549*, 374−378.
(15) Katsonis, N.; Lubomska, M.; Pollard, M. M.; Feringa, B. L.; Rudolf, P. Synthetic Light-Activated Molecular Switches and Motors on Surfaces. *Prog. Surf. Sci.* **2007**, *82*, 407−434.
(16) Broichhagen, J.; Frank, J. A.; Trauner, D. A Roadmap to Success in Photopharmacology. *Acc. Chem. Res.* **2015**, *48*, 1947−1960.
(17) Weston, C. E.; Krämer, A.; Colin, F.; Yildiz, Ö.; Baud, M. G. J.; Meyer-Almes, F.-J.; Fuchter, M. J. Toward Photopharmacological Antimicrobial Chemotherapy Using Photoswitchable Amidohydrolase Inhibitors. *ACS Infect. Dis.* **2017**, *3*, 152−161.
(18) Fiedler, D.; Leung, D.; Bergman, R.; Raymond, K. Selective Molecular Recognition, C-H Bond Activation, and Catalysis in Nanoscale Reaction Vessels. *Acc. Chem. Res.* **2005**, *38*, 349−358.
(19) Tripp, B. C.; Smith, K.; Ferry, J. G. Carbonic Anhydrase: New Insights for an Ancient Enzyme. *J. Biol. Chem.* **2001**, *276*, 48615−48618.
(20) Zhang, X.; Houk, K. N. Why Enzymes Are Proficient Catalysts: Beyond the Pauling Paradigm. *Acc. Chem. Res.* **2005**, *38*, 379−385.
(21) Whicher, J. R.; Dutta, S.; Hansen, D. A.; Hale, W. A.; Chemler, J. A.; Dosey, A. M.; Narayan, A. R. H.; Håkansson, K.; Sherman, D. H.; Smith, J. L.; Skiniotis, G. Structural Rearrangements of a Polyketide Synthase Module during Its Catalytic Cycle. *Nature* **2014**, *510*, 560−564.
(22) Grommet, A. B.; Feller, M.; Klajn, R. Chemical Reactivity under Nanoconfinement. *Nat. Nanotechnol.* **2020**, *15*, 256−271.
(23) Janiak, C.; Vieth, J. K. MOFs, MILs and More: Concepts, Properties and Applications for Porous Coordination Networks (PCNs). *New J. Chem.* **2010**, *34*, 2366−2388.
(24) Goettmann, F.; Sanchez, C. How Does Confinement Affect the Catalytic Activity of Mesoporous Materials? *J. Mater. Chem.* **2007**, *17*, 24−30.
(25) Boyd, P. G.; Chidambaram, A.; García-Díez, E.; Ireland, C. P.; Daff, T. D.; Bounds, R.; Gładysiak, A.; Schouwink, P.; Moosavi, S. M.; Maroto-Valer, M. M.; Reimer, J. A.; Navarro, J. A. R.; Woo, T. K.; Garcia, S.; Stylianou, K. C.; Smit, B. Data-Driven Design of Metal−Organic Frameworks for Wet Flue Gas CO_2 Capture. *Nature* **2019**, *576*, 253−256.
(26) Chu, Z.; Han, Y.; Bian, T.; De, S.; Král, P.; Klajn, R. Supramolecular Control of Azobenzene Switching on Nanoparticles. *J. Am. Chem. Soc.* **2019**, *141*, 1949−1960.
(27) Ahrens, J.; Bian, T.; Vexler, T.; Klajn, R. Irreversible Bleaching of Donor−Acceptor Stenhouse Adducts on the Surfaces of Magnetite Nanoparticles. *ChemPhotoChem.* **2017**, *1*, 230−236.
(28) Zdobinsky, T.; Sankar Maiti, P.; Klajn, R. Support Curvature and Conformational Freedom Control Chemical Reactivity of Immobilized Species. *J. Am. Chem. Soc.* **2014**, *136*, 2711−2714.
(29) Zhao, H.; Sen, S.; Udayabhaskararao, T.; Sawczyk, M.; Kučanda, K.; Manna, D.; Kundu, P. K.; Lee, J.-W.; Král, P.; Klajn, R. Reversible Trapping and Reaction Acceleration within Dynamically Self-Assembling Nanoflasks. *Nat. Nanotechnol.* **2016**, *11*, 82−88.
(30) Fallah-Araghi, A.; Meguellati, K.; Baret, J.-C.; Harrak, A. E.; Mangeat, T.; Karplus, M.; Ladame, S.; Marques, C. M.; Griffiths, A. D. Enhanced Chemical Synthesis at Soft Interfaces: A Universal Reaction-Adsorption Mechanism in Microcompartments. *Phys. Rev. Lett.* **2014**, *112*, No. 028301.
(31) Franco, C.; Rodríguez-San-Miguel, D.; Sorrenti, A.; Sevim, S.; Pons, R.; Platero-Prats, A. E.; Pavlovic, M.; Szilágyi, I.; Ruiz Gonzalez, M. L.; González-Calbet, J. M.; Bochicchio, D.; Pesce, L.; Pavan, G. M.; Imaz, I.; Cano-Sarabia, M.; Maspoch, D.; Pané, S.; de Mello, A. J.; Zamora, F.; Puigmartí-Luis, J. Biomimetic Synthesis of Sub-20 nm Covalent Organic Frameworks in Water. *J. Am. Chem. Soc.* **2020**, *142*, 3540−3547.
(32) Zhang, G.; Mastalerz, M. Organic Cage Compounds − from Shape-Persistency to Function. *Chem. Soc. Rev.* **2014**, *43*, 1934−1947.
(33) Kang, J.; Rebek, J. Acceleration of a Diels−Alder Reaction by a Self-Assembled Molecular Capsule. *Nature* **1997**, *385*, 50−52.
(34) Yoshizawa, M.; Klosterman, J. K.; Fujita, M. Functional Molecular Flasks: New Properties and Reactions within Discrete, Self-Assembled Hosts. *Angew. Chem., Int. Ed.* **2009**, *48*, 3418−3438.
(35) Roy, B.; Ghosh, A. K.; Srivastava, S.; D'Silva, P.; Mukherjee, P. S. A Pd_8 Tetrafacial Molecular Barrel as Carrier for Water Insoluble Fluorophore. *J. Am. Chem. Soc.* **2015**, *137*, 11916−11919.
(36) Wang, K.; Cai, X.; Yao, W.; Tang, D.; Kataria, R.; Ashbaugh, H. S.; Byers, L. D.; Gibb, B. C. Electrostatic Control of Macrocyclization Reactions within Nanospaces. *J. Am. Chem. Soc.* **2019**, *141*, 6740−6747.
(37) Cook, T. R.; Stang, P. J. Recent Developments in the Preparation and Chemistry of Metallacycles and Metallacages via Coordination. *Chem. Rev.* **2015**, *115*, 7001−7045.
(38) Sepehrpour, H.; Fu, W.; Sun, Y.; Stang, P. J. Biomedically Relevant Self-Assembled Metallacycles and Metallacages. *J. Am. Chem. Soc.* **2019**, *141*, 14005−14020.
(39) Liu, M.; Zhang, L.; Little, M. A.; Kapil, V.; Ceriotti, M.; Yang, S.; Ding, L.; Holden, D. L.; Balderas-Xicohténcatl, R.; He, D.; Clowes, R.; Chong, S. Y.; Schütz, G.; Chen, L.; Hirscher, M.; Cooper, A. I. Barely Porous Organic Cages for Hydrogen Isotope Separation. *Science* **2019**, *366*, 613−620.
(40) Merget, S.; Catti, L.; Piccini, G.; Tiefenbacher, K. Requirements for Terpene Cyclizations inside the Supramolecular Resorcinarene Capsule: Bound Water and Its Protonation Determine the Catalytic Activity. *J. Am. Chem. Soc.* **2020**, *142*, 4400−4410.
(41) Yoshizawa, M.; Tamura, M.; Fujita, M. Diels-Alder in Aqueous Molecular Hosts: Unusual Regioselectivity and Efficient Catalysis. *Science* **2006**, *312*, 251−254.
(42) Ueda, Y.; Ito, H.; Fujita, D.; Fujita, M. Permeable Self-Assembled Molecular Containers for Catalyst Isolation Enabling Two-Step Cascade Reactions. *J. Am. Chem. Soc.* **2017**, *139*, 6090−6093.
(43) Maestri, M.; Iglesia, E. First-Principles Theoretical Assessment of Catalysis by Confinement: $NO-O_2$ Reactions within Voids of Molecular Dimensions in Siliceous Crystalline Frameworks. *Phys. Chem. Chem. Phys.* **2018**, *20*, 15725−15735.
(44) Mal, P.; Breiner, B.; Rissanen, K.; Nitschke, J. R. White Phosphorus Is Air-Stable Within a Self-Assembled Tetrahedral Capsule. *Science* **2009**, *324*, 1697.
(45) Yamashina, M.; Sei, Y.; Akita, M.; Yoshizawa, M. Safe Storage of Radical Initiators within a Polyaromatic Nanocapsule. *Nat. Commun.* **2014**, *5*, 4662.

https://dx.doi.org/10.1021/jacs.0c03444
J. Am. Chem. Soc. 2020, 142, 9792−9802

(46) Galan, A.; Ballester, P. Stabilization of Reactive Species by Supramolecular Encapsulation. *Chem. Soc. Rev.* **2016**, *45*, 1720−1737.
(47) Qiu, Y.; Antony, L. W.; Torkelson, J. M.; de Pablo, J. J.; Ediger, M. D. Tenfold Increase in the Photostability of an Azobenzene Guest in Vapor-Deposited Glass Mixtures. *J. Chem. Phys.* **2018**, *149*, 204503.
(48) Qiu, Y.; Antony, L. W.; de Pablo, J. J.; Ediger, M. D. Photostability Can Be Significantly Modulated by Molecular Packing in Glasses. *J. Am. Chem. Soc.* **2016**, *138*, 11282−11289.
(49) Fregoni, J.; Granucci, G.; Persico, M.; Corni, S. Strong Coupling with Light Enhances the Photoisomerization Quantum Yield of Azobenzene. *Chem.* **2020**, *6*, 250−265.
(50) Bochicchio, D.; Kwangmettatam, S.; Kudernac, T.; Pavan, G. M. How Defects Control the Out-of-Equilibrium Dissipative Evolution of a Supramolecular Tubule. *ACS Nano* **2019**, *13*, 4322−4334.
(51) Kusukawa, T.; Fujita, M. Ship-in-a-Bottle" Formation of Stable Hydrophobic Dimers of *Cis*-Azobenzene and -Stilbene Derivatives in a Self-Assembled Coordination Nanocage. *J. Am. Chem. Soc.* **1999**, *121*, 1397−1398.
(52) Cantatore, V.; Granucci, G.; Rousseau, G.; Padula, G.; Persico, M. Photoisomerization of Self-Assembled Monolayers of Azobiphenyls: Simulations Highlight the Role of Packing and Defects. *J. Phys. Chem. Lett.* **2016**, *7*, 4027−4031.
(53) Clever, G. H.; Tashiro, S.; Shionoya, M. Light-Triggered Crystallization of a Molecular Host-Guest Complex. *J. Am. Chem. Soc.* **2010**, *132*, 9973−9975.
(54) Dube, H.; Ajami, D.; Rebek, J. Photochemical Control of Reversible Encapsulation. *Angew. Chem., Int. Ed.* **2010**, *49*, 3192−3195.
(55) Mohan Raj, A.; Raymo, F. M.; Ramamurthy, V. Reversible Disassembly−Assembly of Octa Acid−Guest Capsule in Water Triggered by a Photochromic Process. *Org. Lett.* **2016**, *18*, 1566−1569.
(56) Yang, Y.; Hughes, R. P.; Aprahamian, I. Visible Light Switching of a BF_2-Coordinated Azo Compound. *J. Am. Chem. Soc.* **2012**, *134*, 15221−15224.
(57) Helmy, S.; Leibfarth, F. A.; Oh, S.; Poelma, J. E.; Hawker, C. J.; Read de Alaniz, J. Photoswitching Using Visible Light: A New Class of Organic Photochromic Molecules. *J. Am. Chem. Soc.* **2014**, *136*, 8169−8172.
(58) Zhang, D.; Ronson, T. K.; Mosquera, J.; Martinez, A.; Guy, L.; Nitschke, J. R. Anion Binding in Water Drives Structural Adaptation in an Azaphosphatrane-Functionalized $Fe^{II}_4L_4$ Tetrahedron. *J. Am. Chem. Soc.* **2017**, *139*, 6574−6577.
(59) Rizzuto, F. J.; Nitschke, J. R. Stereochemical Plasticity Modulates Cooperative Binding in a $Co^{II}_{12}L_6$ Cuboctahedron. *Nat. Chem.* **2017**, *9*, 903−908.
(60) Mondal, P.; Sarkar, S.; Rath, S. P. Cyclic Bis-Porphyrin-Based Flexible Molecular Containers: Controlling Guest Arrangements and Supramolecular Catalysis by Tuning Cavity Size. *Chem. - Eur. J.* **2017**, *23*, 7093−7103.
(61) Samanta, D.; Mukherjee, S.; Patil, Y. P.; Mukherjee, P. S. Self-Assembled Pd_6 Open Cage with Triimidazole Walls and the Use of Its Confined Nanospace for Catalytic Knoevenagel- and Diels−Alder Reactions in Aqueous Medium. *Chem. - Eur. J.* **2012**, *18*, 12322−12329.
(62) Samanta, D.; Gemen, J.; Chu, Z.; Diskin-Posner, Y.; Shimon, L. J. W.; Klajn, R. Reversible Photoswitching of Encapsulated Azobenzenes in Water. *Proc. Natl. Acad. Sci. U. S. A.* **2018**, *115*, 9379−9384.
(63) Samanta, D.; Galaktionova, D.; Gemen, J.; Shimon, L. J. W.; Diskin-Posner, Y.; Avram, L.; Král, P.; Klajn, R. Reversible Chromism of Spiropyran in the Cavity of a Flexible Coordination Cage. *Nat. Commun.* **2018**, *9*, 641.
(64) Hanopolskyi, A. I.; De, S.; Białek, M. J.; Diskin-Posner, Y.; Avram, L.; Feller, M.; Klajn, R. Reversible Switching of Arylazopyrazole within a Metal−Organic Cage. *Beilstein J. Org. Chem.* **2019**, *15*, 2398−2407.
(65) Böckmann, M.; Peter, C.; Site, L. D.; Doltsinis, N. L.; Kremer, K.; Marx, D. Atomistic Force Field for Azobenzene Compounds Adapted for QM/MM Simulations with Applications to Liquids and Liquid Crystals. *J. Chem. Theory Comput.* **2007**, *3*, 1789−1802.
(66) Peter, C.; Site, L. D.; Kremer, K. Classical Simulations from the Atomistic to the Mesoscale and Back: Coarse Graining an Azobenzene Liquid Crystal. *Soft Matter* **2008**, *4*, 859−869.
(67) Ilnytskyi, J. M.; Slyusarchuk, A.; Saphiannikova, M. Photocontrollable Self-Assembly of Azobenzene-Decorated Nanoparticles in Bulk: Computer Simulation Study. *Macromolecules* **2016**, *49*, 9272−9282.
(68) Osella, S.; Minoia, A.; Beljonne, D. Combined Molecular Dynamics and Density Functional Theory Study of Azobenzene−Graphene Interfaces. *J. Phys. Chem. C* **2016**, *120*, 6651−6658.
(69) Döbbelin, M.; Ciesielski, A.; Haar, S.; Osella, S.; Bruna, M.; Minoia, A.; Grisanti, L.; Mosciatti, T.; Richard, F.; Prasetyanto, E. A.; De Cola, L.; Palermo, V.; Mazzaro, R.; Morandi, V.; Lazzaroni, R.; Ferrari, A. C.; Beljonne, D.; Samorì, P. Light-Enhanced Liquid-Phase Exfoliation and Current Photoswitching in Graphene−Azobenzene Composites. *Nat. Commun.* **2016**, *7*, 11090.
(70) Laio, A.; Parrinello, M. Escaping Free-Energy Minima. *Proc. Natl. Acad. Sci. U. S. A.* **2002**, *99*, 12562−12566.
(71) Pederzoli, M.; Pittner, J.; Barbatti, M.; Lischka, H. Nonadiabatic Molecular Dynamics Study of the *Cis*−*Trans* Photoisomerization of Azobenzene Excited to the S1 State. *J. Phys. Chem. A* **2011**, *115*, 11136−11143.
(72) Tiago, M. L.; Ismail-Beigi, S.; Louie, S. G. Photoisomerization of Azobenzene from First-Principles Constrained Density-Functional Calculations. *J. Chem. Phys.* **2005**, *122*, No. 094311.
(73) Bochicchio, D.; Salvalaglio, M.; Pavan, G. M. Into the Dynamics of a Supramolecular Polymer at Submolecular Resolution. *Nat. Commun.* **2017**, *8*, 147.
(74) Tiwary, P.; Parrinello, M. From Metadynamics to Dynamics. *Phys. Rev. Lett.* **2013**, *111*, 230602.
(75) Pace, G.; Ferri, V.; Grave, C.; Elbing, M.; von Hänisch, C.; Zharnikov, M.; Mayor, M.; Rampi, M. A.; Samorì, P. Cooperative Light-Induced Molecular Movements of Highly Ordered Azobenzene Self-Assembled Monolayers. *Proc. Natl. Acad. Sci. U. S. A.* **2007**, *104*, 9937.
(76) Titov, E.; Granucci, G.; Götze, J. P.; Persico, M.; Saalfrank, P. Dynamics of Azobenzene Dimer Photoisomerization: Electronic and Steric Effects. *J. Phys. Chem. Lett.* **2016**, *7*, 3591−3596.

https://dx.doi.org/10.1021/jacs.0c03444
J. Am. Chem. Soc. 2020, 142, 9792−9802